DOI: 10.31276/VJSTE.66(2).89-100

Molecular docking and molecular dynamics simulation revealed potential compounds in *Salvia miltiorrhiza* for inhibiting enzymes and receptors in Alzheimer's disease

Tung Bui Thanh*, Trang Vu Dai, Huong Le Thi

Pharmacology Department, University of Medicine and Pharmacy, Vietnam National University - Hanoi, 144 Xuan Thuy Street, Dich Vong Hau Ward, Cau Giay District, Hanoi, Vietnam

Received 13 September 2023; revised 8 November 2023; accepted 19 January 2024

Abstract:

Alzheimer's disease is an age-related neurodegenerative disorder that leads to cognitive and functional decline. Potential target proteins for managing Alzheimer's disease include Acetylcholinesterase (AChE), Butyrylcholinesterase (BuChE), Beta-secretase cleavage enzyme (BACE1) and *N*-methyl-D-aspartate (NMDA) receptors. In this study, we conducted *in silico* evaluations of the inhibitory effects of *Salvia miltiorrhiza's* compounds on AChE, BuChE, BACE1, and NMDA receptors. The Lipinski's rule of five was employed to compare phytochemicals with drug-like and non-drug-like properties. Based on previous publications, we compiled a list of 30 compounds from *S. miltiorrhiza* with potential for improving Alzheimer's disease. Among these 30 compounds, six natural compounds exhibited potential inhibition of all four target proteins. Five of these six compounds, namely Tanshinone I, Tanshinone IIA, Isotanshinone I, Dihydroisotanshinone I, and Dihydroisotanshinone II, possessed drug-like properties, good absorption potential, and the ability to cross the blood-brain barrier. In conclusion, these five compounds show the highest potential as future drug candidates for the treatment of Alzheimer's disease.

Keywords: **Alzheimer, *in silico,* molecular docking, molecular dynamics, *Salvia miltiorrhiza*.**

Classification numbers: **3.3, 3.5**

1. Introduction

Alzheimer's disease is an age-related neurodegenerative disorder resulting in cognitive and functional decline. Research has identified three stages of Alzheimer's disease: preclinical Alzheimer's disease, mild cognitive impairment (MCI) due to Alzheimer's disease, and dementia due to Alzheimer's disease. In the first stage, individuals exhibit no symptoms such as memory loss, but they already display early signs of the disease indicated by biomarkers. In the subsequent two stages, clinical symptoms of Alzheimer's disease become more evident. Alongside biomarker evidence, such as increased levels of beta-amyloid, patients with MCI due to Alzheimer's disease experience more pronounced cognitive decline than individuals of the same age. The final stage, dementia due to Alzheimer's disease, is characterized by numerous symptoms related to memory, cognition, and behavior, significantly impairing an individual's daily functioning [1]. Vietnam, one of the world's fastest-aging countries, is witnessing a rising number of people with Alzheimer's disease and related dementias [2].

Therapeutically, Alzheimer's disease management focuses on two primary strategies: symptomatic and mechanism-based therapeutic approaches targeting β-amyloid and tau pathologies.

Firstly, in the strategy for symptomatic improvements, the inhibition of brain cholinesterase activity and the regulation of glutamate activity have been considered the two main treatment avenues for Alzheimer's disease [3].

Inhibition of brain cholinesterases was believed to raise acetylcholine levels since acetylcholine, the neurotransmitter, is rapidly degraded by the hydrolytic activity of cholinesterases following its release into the synaptic cleft [3]. Increasing acetylcholine levels is thought to reduce symptoms of Alzheimer's disease. In the human brain, the most prominent enzyme responsible for acetylcholine hydrolysis is AChE. AChE plays a vital role in catalysing the breakdown of acetylcholine into choline and acetic acid, a reaction necessary for cholinergic neurons to return to their resting state after activation [4]. Another study suggests that BuChE may also hydrolyse acetylcholine in the brain, contributing to cholinergic transmission [5]. Therefore, inhibiting these two enzymes is considered a therapeutic approach to enhancing cognitive and neural cell function.

The other therapy to improve Alzheimer's disease symptoms involves regulating glutamate activity. Glutamate excitotoxicity, mediated through excessive activation of NMDA receptors, has been linked to neuronal death observed in Alzheimer's disease and other neurodegenerative conditions [3]. This results in neuronal cell death and a decline in cognitive function. Consequently, NMDA receptor antagonists are believed to alleviate Alzheimer's disease symptoms by preventing glutamate-mediated neurotoxicity.

Second are mechanism-based therapeutic approaches targeting β-amyloid and tau pathologies. Alzheimer's disease is characterized by the presence of extracellular amyloid β

*Corresponding author: Email: tungbt.ump@vnu.edu.vn

(Aβ) plaques and intracellular deposition of neurofibrillary tangles (NFTs) [3, 6]. Aβ is an aggregated form of amyloid β peptide, while NFTs consist of hyperphosphorylated tau proteins. BACE1 plays a crucial role in producing amyloid-β proteins by cleaving proteins from amyloid precursor proteins, leading to neurotoxicity and neuronal death [7, 8]. Therefore, inhibiting BACE1 to prevent Aβ production holds potential as a therapy for Alzheimer's disease. In this study, we selected AChE, BuChE, NMDA receptor, and BACE1 as target proteins.

Molecular docking is a widely used computational structure-based drug design (SBDD) method that has been employed since the early 1980s [9]. Molecular docking aims to predict the most favourable position and configuration for a substrate molecule to bind to a protein. This method simplifies the identification of compounds with the best pharmacological effects without the need for experiments. Additionally, this *in silico* method saves considerable time, cost, and effort [10].

Salvia miltiorrhiza Bunge belongs to the *Salvia* Linn. genus, the largest in the Lamiaceae family. S. *miltiorrhiza*, native to China and Japan, is primarily produced in China, with smaller production areas in countries like Japan and Vietnam. In Vietnam, S. *miltiorrhiza* thrives in the northern regions. *Salvia miltiorrhiza* Bunge is a well-known traditional herb with a history of use in preventing and treating various ailments, including neurological diseases, cancer, inflammation, and cardiovascular diseases [11].

In this study, we employed *in silico* techniques to identify natural compounds from *Salvia miltiorrhiza* Bunge that could potentially be effective in treating Alzheimer's disease and other neurodegenerative disorders.

2. Materials and methods

2.1. Retrieval and preparation of protein structure

Initially, the three-dimensional (3D) structures of the NMDA receptor (PDB ID: 1PBQ), enzyme β-secretase 1 (PDB ID: 4X7I), enzyme BuChE (PDB ID: 4BDS), and enzyme AChE (PDB ID: 1EVE) were obtained from the Protein Data Bank RCSB. Subsequently, all water molecules and co-crystallised ligands were removed from the protein structures using Discovery Studio Visualizer v21.1.0.20298 software. MGL Autodock Tools 1.5.6 software was utilised to regenerate the active site after supplying missing hydrogen atoms with Autodock Vina. Finally, these proteins were saved in pdbqt format in preparation for the docking program.

2.2. Ligands preparation

Based on prior publications, we gathered 30 compounds from S. *miltiorrhiza* with potential to improve Alzheimer's disease (Table 1). Next, the 3D structures were obtained from PubChem in SDF format and then converted into PDB format using Chimera 1.17.3 software. Subsequently, these structures were optimised using Avogadro 1.2.0 software with conjugate gradients and converted to PDBQT format using Autodock Tools software.

Table 1. Structures of the 30 compounds from *S. miltiorrhiza*.

No	Name	Molecular formula	No	Name	Molecular formula
1	Tanshinone I	$C_{18}H_{12}O_3$	16	4-Methylenemiltirone	$C_{18}H_{18}O_2$
2	Tanshinol A	$C_{18}H_{12}O_4$	17	Caffeic acid	$C_9H_8O_4$
3	Przewaquinone B	$C_{18}H_{12}O_4$	18	Isotanshinone I	$C_{18}H_{12}O_3$
4	Tanshinone IIA	$C_{19}H_{18}O_3$	19	Dihydroisotanshinone I	$C_{18}H_{14}O_3$
5	Hydroxytanshinone IIA	$C_{19}H_{18}O_4$	20	Dihydroisotanshinone II	$C_{18}H_{14}O_3$
6	Tanshinone IIB	$C_{19}H_{18}O_4$	21	Danshexinkun A	$C_{18}H_{16}O_4$
7	Danshensu	$C_9H_{10}O_5$	22	Danshenxinkun B	$C_{18}H_{16}O_3$
8	Methyl tanshinonate	$C_{20}H_{18}O_5$	23	Danshenxinkun C	$C_{16}H_{12}O_3$
9	Tanshinaldehyde	$C_{19}H_{18}O_4$	24	Isoferulic acid	$C_{10}H_{10}O_4$
10	Tanshindiol A	$C_{18}H_{16}O_5$	25	Salvianolic acid F	$C_{17}H_{14}O_6$
11	Rosmarinic acid	$C_{18}H_{16}O_8$	26	Salvianolic acid G	$C_{18}H_{12}O_7$
12	Przewaquinone A	$C_{19}H_{18}O_4$	27	Sugiol	$C_{20}H_{28}O_2$
13	Tanshindiol C	$C_{18}H_{16}O_5$	28	Sibiriquinone A	$C_{19}H_{20}O_2$
14	Methyl dihydronortanshinonate	$C_{20}H_{20}O_5$	29	Trijuganone B	$C_{18}H_{16}O_3$
15	Miltirone	$C_{19}H_{22}O_2$	30	Neo-przewaquinone A	$C_{36}H_{28}O_6$

2.3. Molecular docking study

The selected phytochemicals were docked into the active sites of proteins using Autodock Vina software. The scoring function of Autodock Vina was employed to calculate the energy of the ligand-protein interactions. Molecular interactions between proteins and the selected compounds with higher binding affinity were visualised using Discovery Studio Visualizer v21.1.0.20298.

2.4. Validation of docking protocol

After separating the co-crystallised ligands from the proteins using Discovery Studio Visualizer v21.1.0.20298 software, the molecules in PDB format were saved and converted to PDBQT format. Subsequently, a re-docking process was carried out where the co-crystallised ligands were re-docked into the active sites of targets prior to screening. The procedure was considered successful if the root mean square deviation (RMSD) value was not higher than 1.5 Å [9].

2.5. Lipinski's rule of five

Lipinski's rule of five is a technique used to compare drug-like molecules and those that are not. It is employed to screen molecules with potential pharmacological profiles similar to drugs. In this study, an online tool was used to evaluate Lipinski's rule of five. The chemical structures were retrieved from the PubChem database and set at pH 7.0.

2.6. Prediction of ADMET by computational analysis

ADMET profiling was employed to assess the physicochemical efficiency of inhibiting the target proteins. Only compounds that satisfy Lipinski's rule of five were evaluated by ADMET profiling. ADMET profile predicts five parameters: absorption, distribution, metabolism, excretion, and toxicity, which are crucial for determining a drug's potential success. Standard ranges for these criteria were

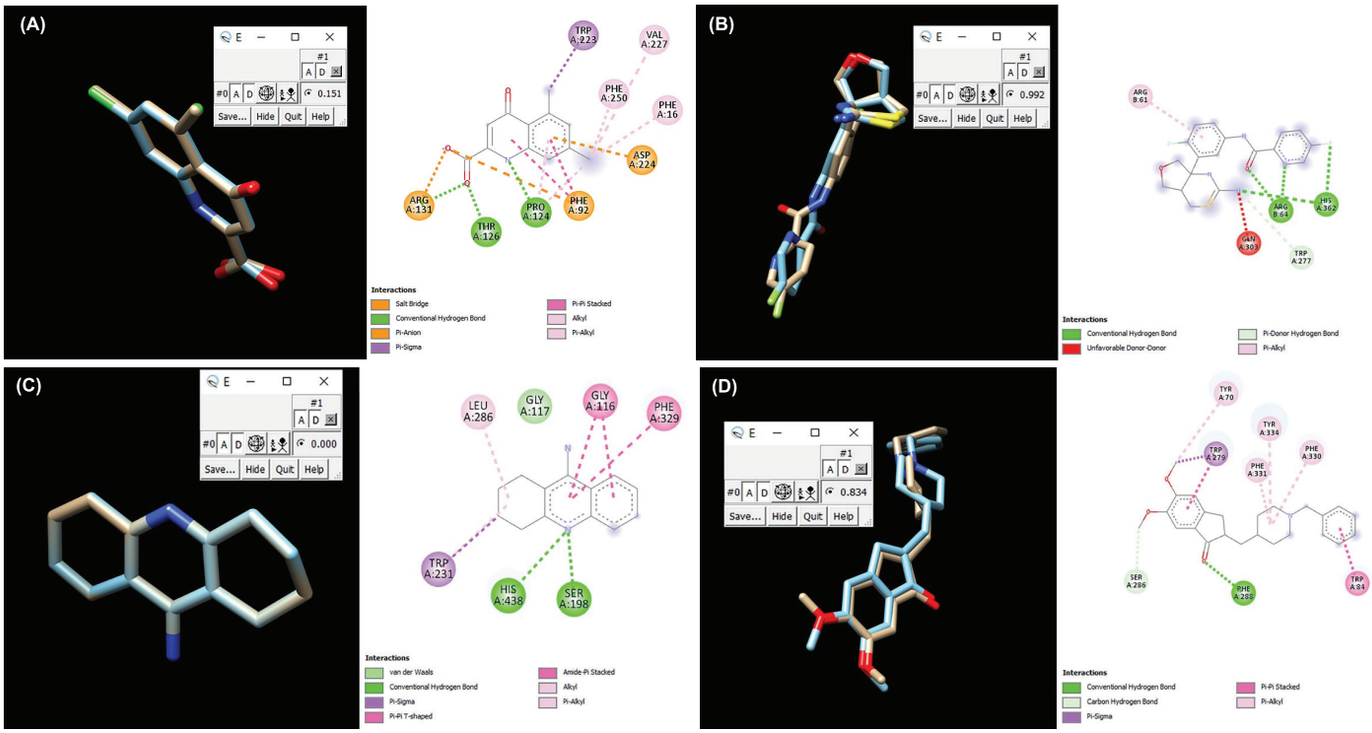

Fig. 1. Results of re-docking and interactions of the co-crystallised ligands with proteins. (A) Re-docking and interactions of the co-crystallised ligand 5,7-dichloro-4-hydroxyquinoline-2-carboxylic acid with NMDA. **(B)** Re-docking and interactions of the co-crystallised ligand LY2886721 with BACE1. **(C)** Re-docking and interactions of the co-crystallised ligand Tacrine with BuChE. **(D)** Re-docking and interactions of the co-crystallised ligand Donepezil with AChE.

tested for compliance, and ADMET profiling was predicted using the pkCSM tool. Canonical SMILES molecular structures of collected phytochemicals were retrieved from PubChem.

2.7. Molecular dynamics simulation of the most potent compounds

Molecular dynamics was employed to assess the physical movement and interactions of all atoms in the protein-ligand complexes, including their interactions with the surroundings. MOE version 2015.10 was used for molecular dynamics (MD) simulations of the complexes with the least binding energy pose. The Nosé-Poincaré-Andersen (NPA) equations of motion were applied in MOE dynamics simulation. The system was optimised for equilibrium over 600 ps, followed by a production run at 310 K for 500 ps. The RMSD was determined using the formula:

$$\text{RMSD} = \sqrt{\frac{1}{N}\sum_{i=1}^{N} di^2}$$

where N is the total number of atoms in the complex and di is the distance between atom i at two separate times.

3. Results

3.1. The result of a validation

Before proceeding with screening, it is crucial to validate the docking protocol. To achieve this, the co-crystallised ligand was extracted from the protein and then re-docked into the active site of the target. The RMSD was calculated, and the structural similarity was assessed using Chimera 1.17.3 software. The superposition of the co-crystallised ligand structures before and after docking with NMDA, BACE1, BuChE, and AChE resulted in RMSD values of 0.151 Å, 0.992 Å, 0 Å, and 0.834 Å, respectively. All RMSD values were found to be less than 1.5 Å, indicating the reliability of the molecular docking outcomes. The results of the re-dock and interactions between the co-crystallised ligands and proteins are presented in Fig. 1.

As depicted in Fig. 1, the co-crystallised ligand 5,7-dichloro-4-hydroxyquinoline-2-carboxylic acid displayed interactions with TRP 223, PHE 250, VAL 227, PHE 16, ASP 224, PHE 92, PRO 124, THR 126, and ARG 131 of NMDA. For BACE1, the co-crystallised ligand LY2886721 interacted with ARG 61, HIS 362, ARG 64, and GLN 303 of the target protein. Tacrine, on the other hand, interacted with LEU 286, GLY 116, PHE 329, SER 198, HIS 438, and TRP 231, which are amino acids in BuChE. Lastly, in the case of AChE, Donepezil interacted with TYR 70, TRP 279, PHE 331, TYR 334, PHE 330, TRP 84, PHE 288, and SER 286.

3.2. Molecular docking of compounds with the target proteins

Following the preparation of ligands, we conducted docking experiments involving 30 phytochemicals and four target proteins: NMDA, BuChE, AChE, and BACE1. To evaluate the potential of these compounds to inhibit these four target proteins, we compared the docking scores of the ligands with those of four reference drugs: memantine, LY2886721, rivastigmine, and donepezil, respectively. The results are presented in Table 2.

Table 2. Docking results of 6 compounds potential and reference compounds with target proteins.

No	Name	Binding energy with proteins (kcal/mol)			
		1PBQ-NMDA	*4X7I-BACE1*	*4BDS-BuChE*	*1EVE-AChE*
1	Tanshinone I	-9.4	-10.5	-9.8	-11.3
2	Tanshinone IIA	-9.4	-10.3	-10.1	-11.2
3	4-Methylenemiltirone	-8.8	-9.7	-9.1	-11.1
4	Isotanshinone I	-9.9	-10.6	-9.9	-11.1
5	Dihydroisotanshinone I	-10.3	-10.6	-10.3	-11.9
6	Dihydroisotanshinone II	-10.4	-10.4	-10.3	-11.1
+	Memantine	-6.9			
+	LY2886721		-9.0		
+	Rivastigmine			-6.9	
+	Donepezil				-10.9

Memantine, an NMDA receptor antagonist, was FDA-approved in 2013 for managing Alzheimer's disease [12]. Rivastigmine, another drug, is known as a dual BuChE and AChE inhibitor, FDA-approved in 2000 for treating mild to moderate Alzheimer's dementia [13, 14]. Donepezil, an AChE inhibitor, has been used to manage behavioural and cognitive symptoms of Alzheimer's disease and related dementias since its initial FDA approval in 1996. In 2014, its extended-release form was approved in combination with memantine for treating patients in moderate and severe stages of Alzheimer's dementia (Donepezil FDA label). In 2015, a study showed that LY2886721 has the potential to be a BACE1 inhibitor. Experiments on mice, dogs, and humans indicated that LY288672 causes robust central Aβ pharmacodynamic responses [15]. Considering this evidence, these four reference drugs were selected as positive control molecules.

Table 2 presents the docking results of six compounds that simultaneously exhibited lower free energies of binding than all four positive control compounds.

Among the 30 compounds, only six compounds, including Tanshinone I, Tanshinone IIA, 4-methylenemiltirone, Isotanshinone I, Dihydroisotanshinone I, and Dihydroisotanshinone II that potentially inhibited all four target proteins.

Therefore, we have chosen these six compounds for further evaluation of their drug-like properties due to their significant potential to inhibit targets in Alzheimer's treatment.

Table 3 and Figs. 2-7 present the active site residues of the target protein interaction with six potential magnetic compounds.

Table 3. Active site residues of target proteins with compounds from *S. miltiorrhiza*.

No	Compounds	Active site residues atom range			
		1PBQ-NMDA	*4X7I-BACE1*	*4BDS-BuChE*	*1EVE-AChE*
1	Tanshinone I	PHE 250, ARG 131, PHE 92	Asp 62, TYR 60, ARG 61, TRP 277	LEU 286, PHE 329, SER 198, HIS 438, GLY 116	PHE 330, TYR 334
2	Tanshinone IIA	VAL 181, TYR 184, LEU 146	ARG 61, THR 275, TYR 320	SER 287, PHE 329, SER 198, GLY 116, HIS 438, TRP 82	TYR 70, TRP 279
3	4-Methylenemiltirone	ARG 131, SER 180, PHE 92	TYR 71	SER 198, HIS 438, PHE 329, PHE 398, GLY 117, LEU 286, TRP 231, TRP 82	PHE 330, TRP 84, TYR334
4	Isotanshinone I	TYR 184, PHE 246, LEU 146,	TYR 71, ASP 32	GLY 116, HIS 438, PHE 329, SER 198, VAL 288, LEU 286, TRP 231	TYR 334, TRP 279
5	Dihydroisotanshinone I	TRP 223, SER 180,	VAL 361	TRP 82, HIS 438, SER 198, GLY 117, TRP 231, LEU 286, PHE 329, TYR 332, TRP 82	TYR 334, PHE 330, TRP 279
6	Dihydroisotanshinone II	TRP 223, PHE 92, PHE 250	TYR 71, TRP 76	TYR 128, TRP 82, HIS 438	PHE 330, TYR 334, TYR 121

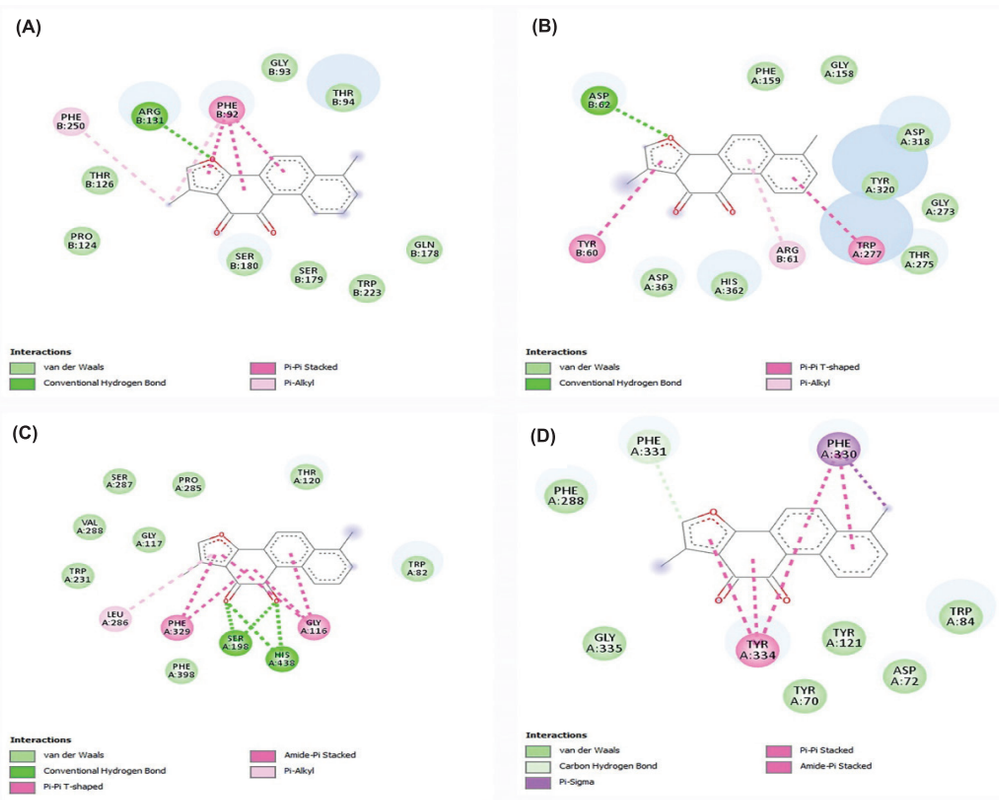

Fig. 2. Binding interactions of Tanshinone I with NMDA (A), BACE1 (B), BuChE (C), and AChE (D).

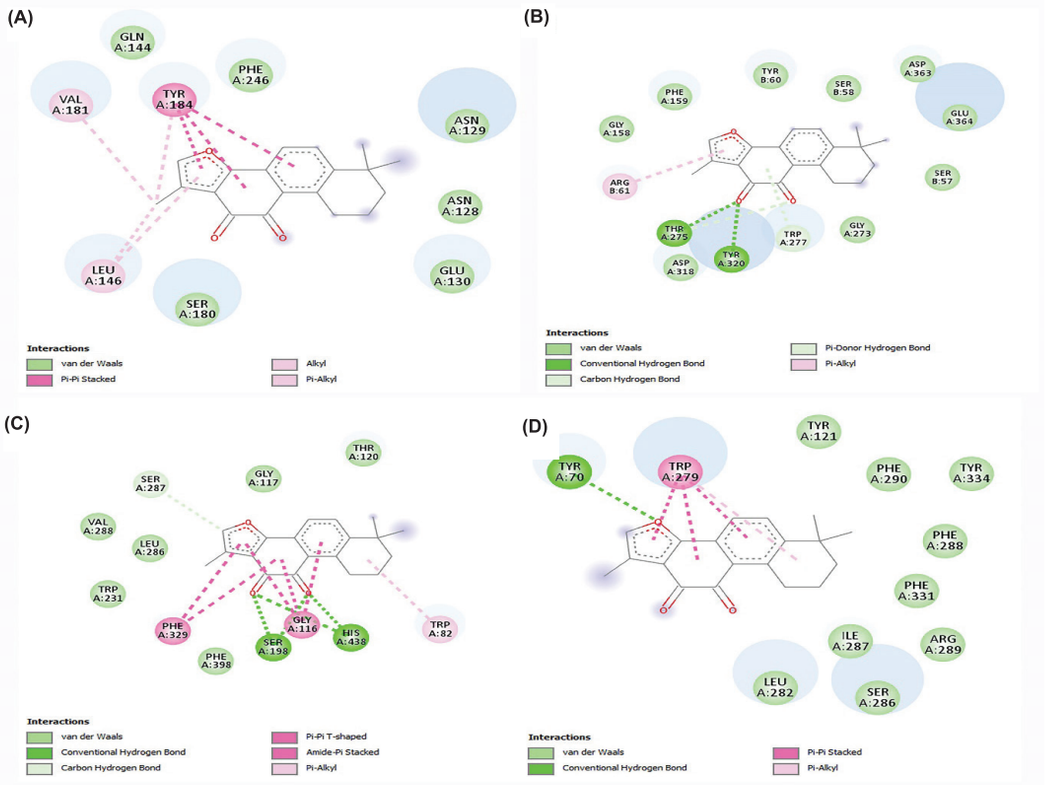

Fig. 3. Binding interactions of Tanshinone IIA with NMDA (A), BACE1 (B), BuChE (C), and AChE (D).

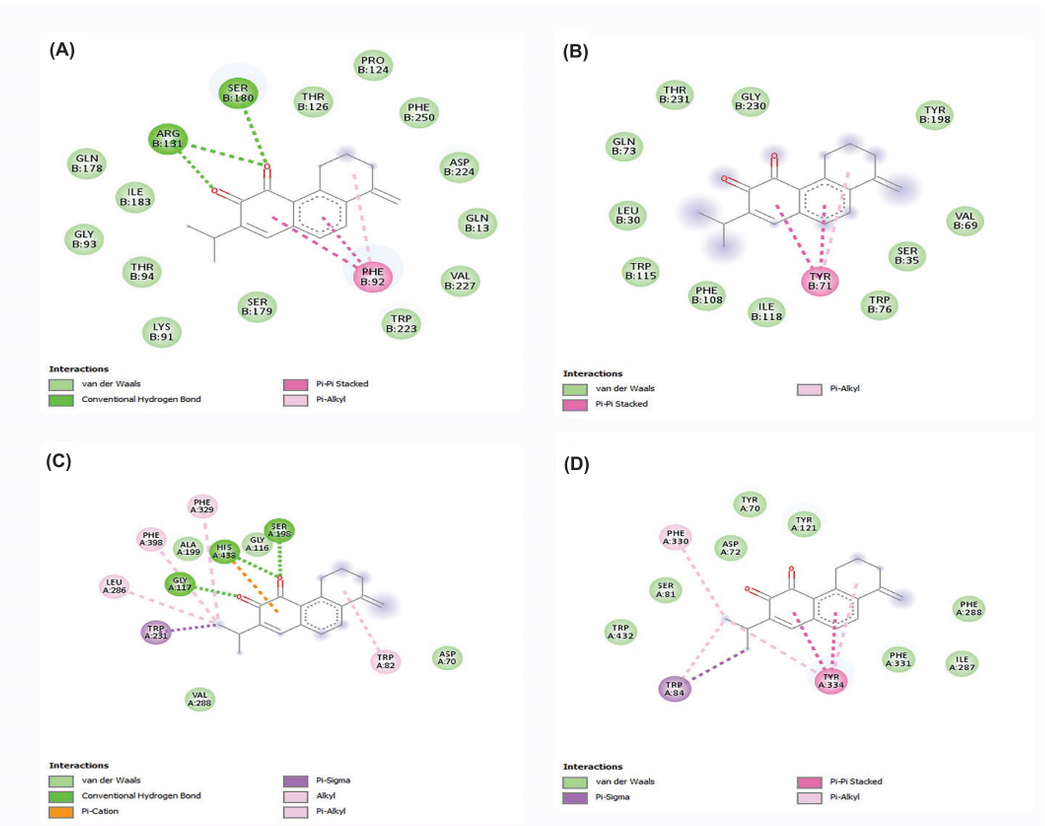

Fig. 4. Binding interactions of 4-Methylenemiltirone with NMDA (A), BACE1 (B), BuChE (C), and AChE (D).

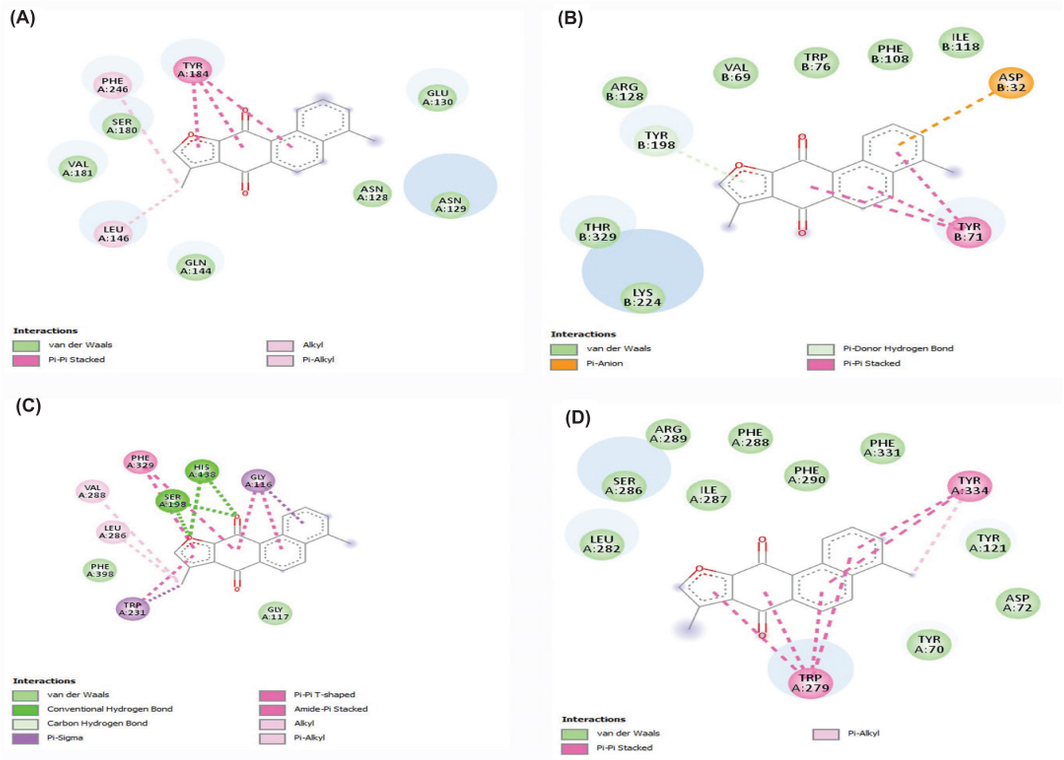

Fig. 5. Binding interactions of Isotanshinone I with NMDA (A), BACE1 (B), BuChE (C), and AChE (D).

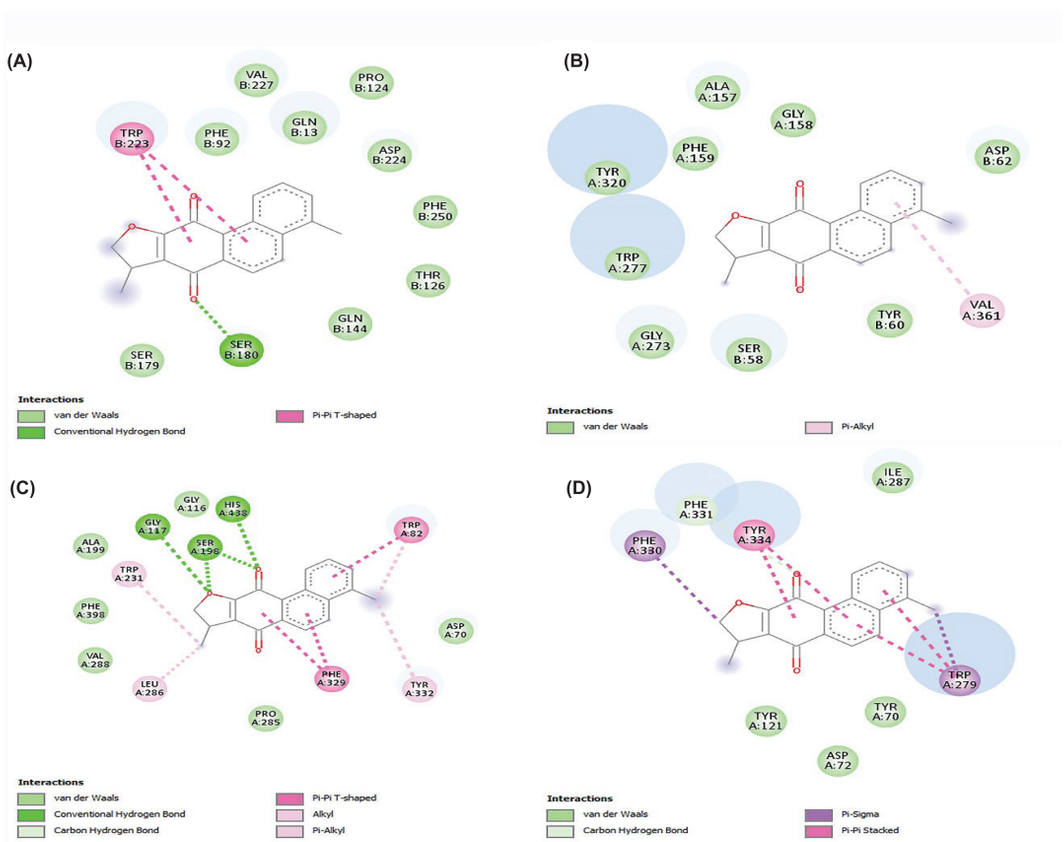

Fig. 6. Binding interactions of Dihydroisotanshinone I with NMDA (A), BACE1 (B), BuChE (C), and AChE (D).

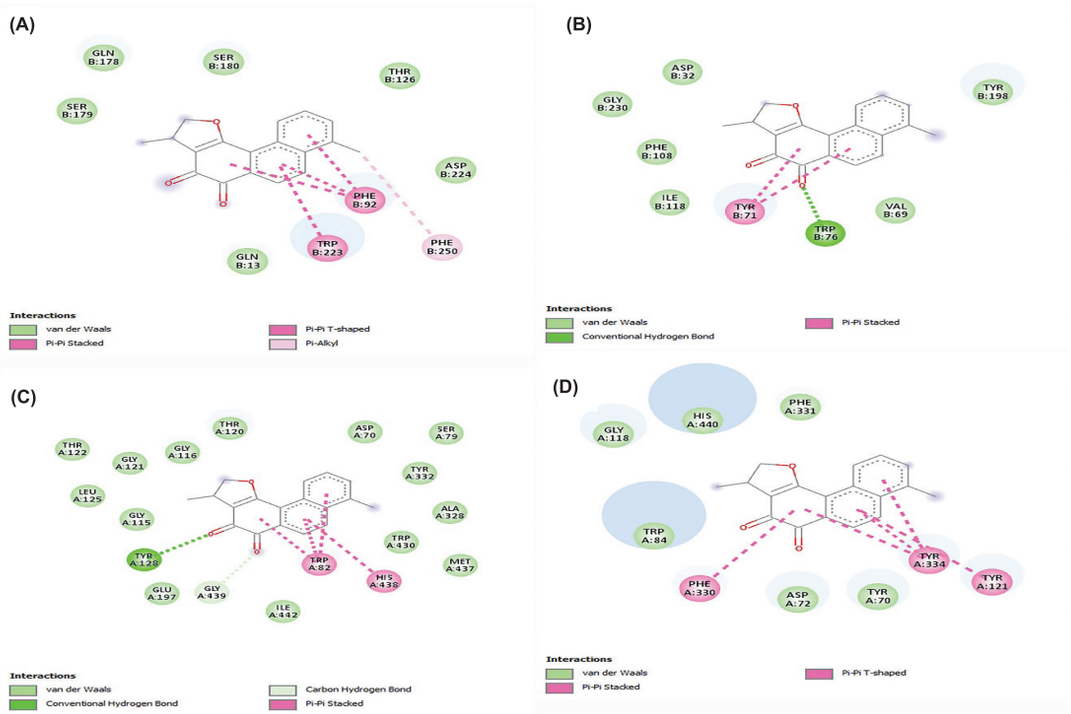

Fig. 7. Binding interactions of Dihydroisotanshinone II with NMDA (A), BACE1 (B), BuChE (C), and AChE (D).

3.3. Lipinski's rule of five

According to Lipinski's rule of five, compounds that satisfy at least two of the following criteria will have the potential to become oral drugs, including: molecular mass (MW) less than 500 Da; high lipophilicity (expressed as LogP less than 5); fewer than 5 hydrogen bond donors (HBD); fewer than 10 hydrogen bond acceptors (HBA1); molar refractivity (MR) between 40 and 130.

The results indicate that all six compounds meet the criteria outlined in Lipinski's rule of five (Table 4).

Table 4. Results of Lipinski's rule of five.

No	Compounds	Molecular weight (Da)	HBD	HBA	Log P	Molar refractivity (MR)	Drug likeness
1	Tanshinone I	276.0	0	3	4.1	79.8	Yes
2	Tanshinone IIA	294.0	0	3	4.2	83.5	Yes
3	4-Methylenemiltirone	266.0	0	3	3.8	80.6	Yes
4	Isotanshinone I	276.0	0	3	3.8	78.9	Yes
5	Dihydroisotanshinone I	278.0	0	3	3.4	79.5	Yes
6	Dihydroisotanshinone II	278.0	0	3	3.3	80.1	Yes

3.4. Prediction of absorption, distribution, metabolism, excretion, and toxicity (ADMET) profile

In silico ADMET profiling was employed to assess the physiochemical efficiency of the six compounds as inhibitors of the target proteins. ADMET profiling predicts five key parameters: absorption, distribution, metabolism, excretion, and toxicity. All five parameters are crucial in determining the likelihood of a compound's success as a drug. Table 5 is the ADMET evaluation results of six potential compounds.

Table 5. ADMET assessment results.

Properties	Tanshinone I	Tanshinone IIA	4-Methylenemiltirone	Isotanshinone I	Dihydroisotanshinone I	Dihydroisotanshinone II
Absorption						
Water solubility (log mol/l)	-4.443	-4.494	-4.986	-4.567	-3.731	-3.883
Caco2 permeability (log Papp in 10^{-6} cm/s)	1.401	1.419	1.774	1.353	1.355	1.366
Intestinal absorption (human) (%)	98.909	96.253	96.635	99.51	99.561	98.628
Distribution						
VDss (human) (log l/kg)	0.561	0.325	0.853	0.629	-0.013	-0.02
BBB permeability (log BB)	0.447	0.302	0.285	0.419	0.56	0.377
Metabolism						
CYP2D6 substrate	No	No	No	No	No	No
CYP3A4 substrate	Yes	Yes	Yes	Yes	Yes	Yes
CYP2D6 inhibitor	No	No	No	No	No	No
CYP3A4 inhibitor	No	No	No	Yes	No	No
Excretion						
Total clearance (log ml/min/kg)	0.209	0.821	0.03	0.15	0.103	0.138
Toxicity						
AMES toxicity	Yes	No	No	Yes	Yes	No
Hepatotoxicity	No	No	Yes	Yes	No	No
Skin sensitisation	No	No	No	No	No	No

In the context of absorption progress, Table 5 shows that the water solubility of all six compounds is notably poor, with concentrations ranging from $10^{-4.9}$ to $10^{-3.7}$ mol/l. CaCo2 membrane permeability (log Papp in 10^{-6} cm/s) with a value higher than 0.9 is indicative of good permeability. Therefore, all six compounds, including Tanshinone I, Tanshinone IIA, 4-methylenemiltirone, Isotanshinone I, Dihydroisotanshinone I, and Dihydroisotanshinone II, are likely to exhibit significant permeability through the CaCo2 cell membrane, with log Papp values of 1.401, 1.419, 1,774, 1.353, 1.355, and 1.366 (in 10^{-6} cm/s), respectively. Additionally, these compounds are predicted to be completely absorbed through the human gut, with absorption rates exceeding 96%.

In terms of distribution, a logBB value greater than 0.3 indicates the likelihood of a compound being absorbed across the blood-brain barrier. The ability to cross the blood-brain barrier is crucial for certain pharmacological effects, such as inhibiting the AChE enzyme. With the exception of 4-methylenemiltirone, the other five compounds have logBB values exceeding 0.3. Tanshinone I and Tanshinone IIA have logBB values of 0.447 and 0.302, while Isotanshinone I, Dihydroisotanshinone I, and Dihydroisotanshinone II have logBB values of 0.419, 0.56, and 0.377, respectively.

Regarding metabolism, cytochrome P450 isozymes play a significant role in drug metabolism in the liver. All six compounds are CYP3A4 substrates, while only Isotanshinone I is a CYP3A4 inhibitor, indicating that they are metabolised by CYP3A4.

The toxicity profile reveals that Tanshinone I, Isotanshinone I, and Dihydroisotanshinone I exhibit AMES toxicity, which assesses the mutagenic potential of chemical compounds. Furthermore, both 4-methylenemiltirone and Isotanshinone I are predicted to cause liver toxicity. Therefore, only Tanshinone IIA and Dihydroisotanshinone II do not exhibit any form of toxicity, including AMES toxicity, hepatotoxicity, and skin sensitisation.

3.5. Molecular dynamics

The ADMET profile results indicate that five compounds, namely Tanshinone I, Tanshinone IIA, Isotanshinone I, Dihydroisotanshinone I, and Dihydroisotanshinone II, are likely to cross the blood-brain barrier, suggesting their potential for managing Alzheimer's disease.

To assess the stability of the docking poses of these five promising compounds, molecular dynamics simulations of the protein-ligand complexes were performed using the docking data as the starting configuration. The molecular dynamics results for all complexes, as depicted in Figs. 8-12, demonstrate that the stable model with free energy reaches equilibrium after approximately 100 ps.

The resulting RMSD values for all complexes are small and generally remain steady. These findings indicate that after 600 ps of molecular dynamics simulation, the positions of the complex's atoms show minimal differences. However, it is essential to further investigate the long-term stability of the protein-ligand complexes.

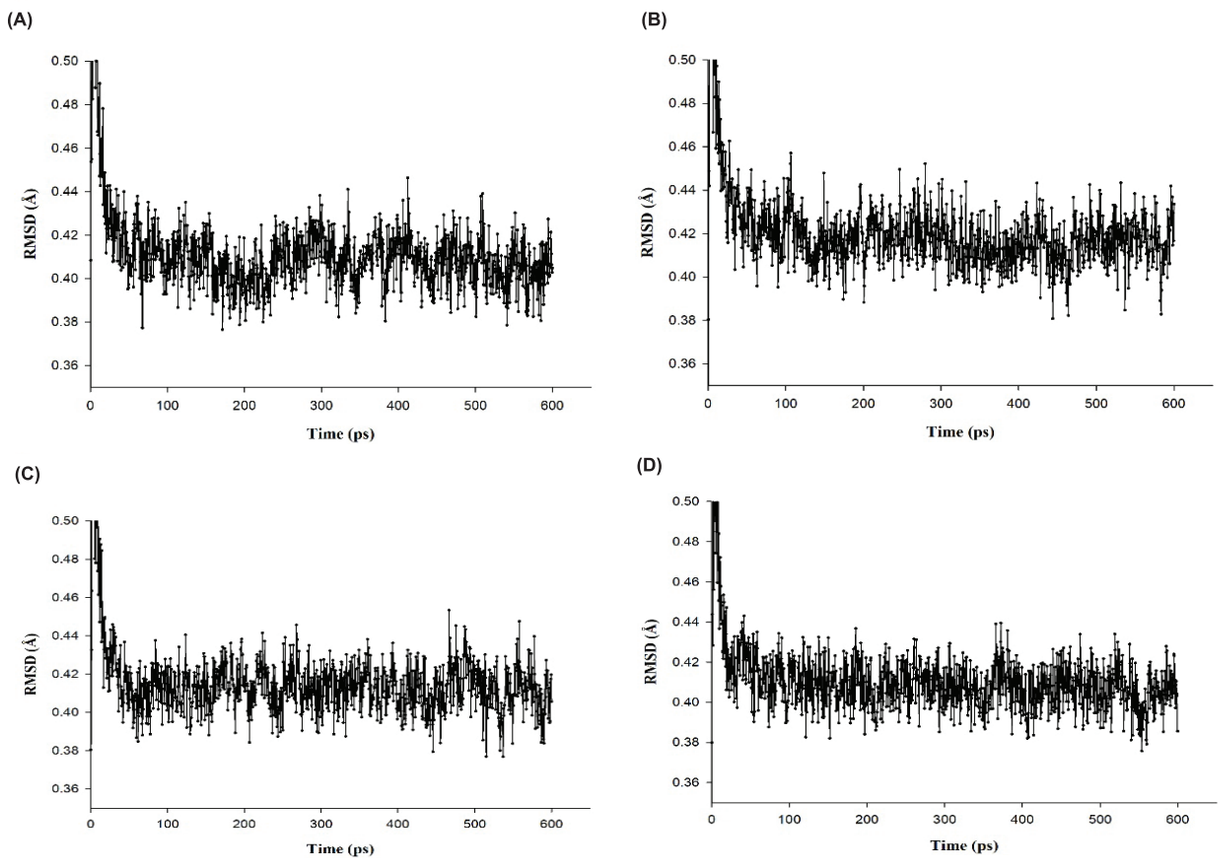

Fig. 8. RMSD of NMDA - Tanshinone I (A), BACE1 - Tanshinone I (B), BuChE - Tanshinone I (C), and AChE - Tanshinone I (D) complexes during 600 ps of molecular dynamics simulation.

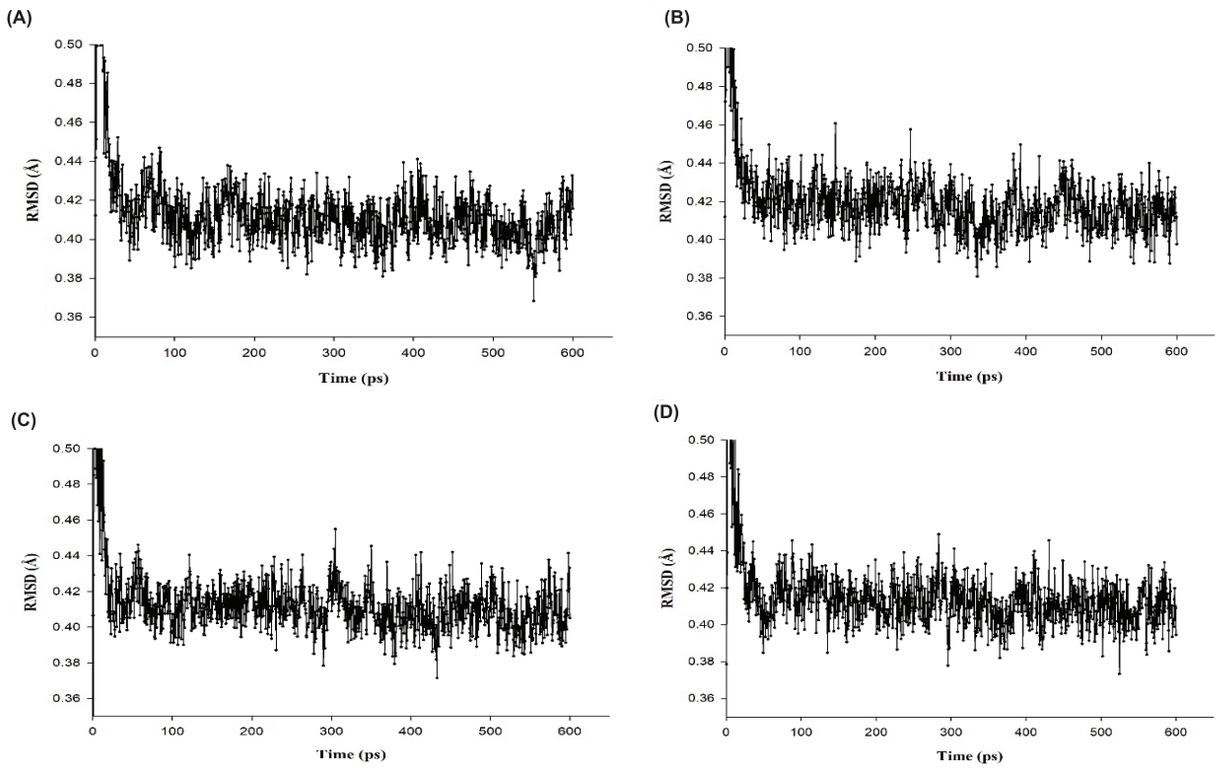

Fig. 9. RMSD of NMDA - Tanshinone IIA (A), BACE1 - Tanshinone IIA (B), BuChE - Tanshinone IIA (C), and AChE - Tanshinone IIA (D) complexes during 600 ps of molecular dynamics simulation.

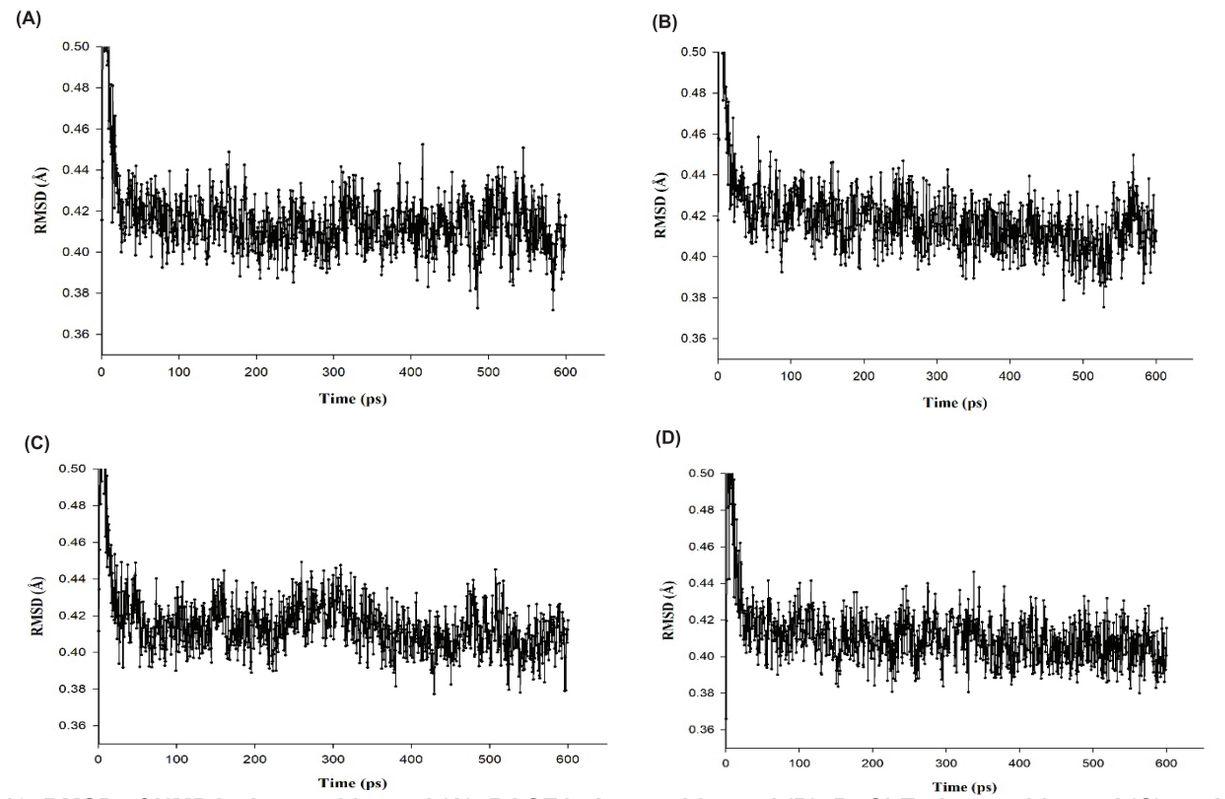

Fig. 10. RMSD of NMDA - Isotanshinone I (A), BACE1 - Isotanshinone I (B), BuChE - Isotanshinone I (C), and AChE - Isotanshinone I (D) complexes during 600 ps of molecular dynamics simulation.

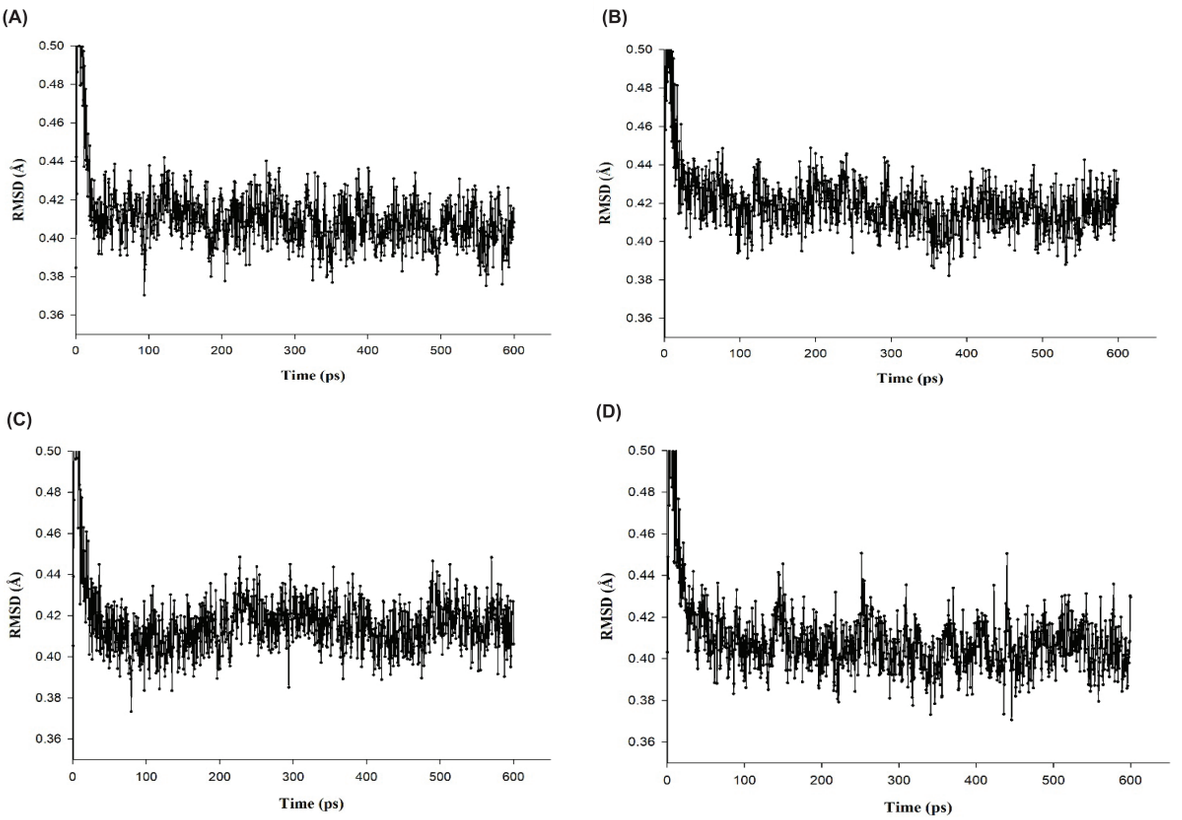

Fig. 11. RMSD of NMDA - Dihydroisotanshinone I (A), BACE1 - Dihydroisotanshinone I (B), BuChE - Dihydroisotanshinone I (C), and AChE - Dihydroisotanshinone I (D) complexes during 600 ps of molecular dynamics simulation.

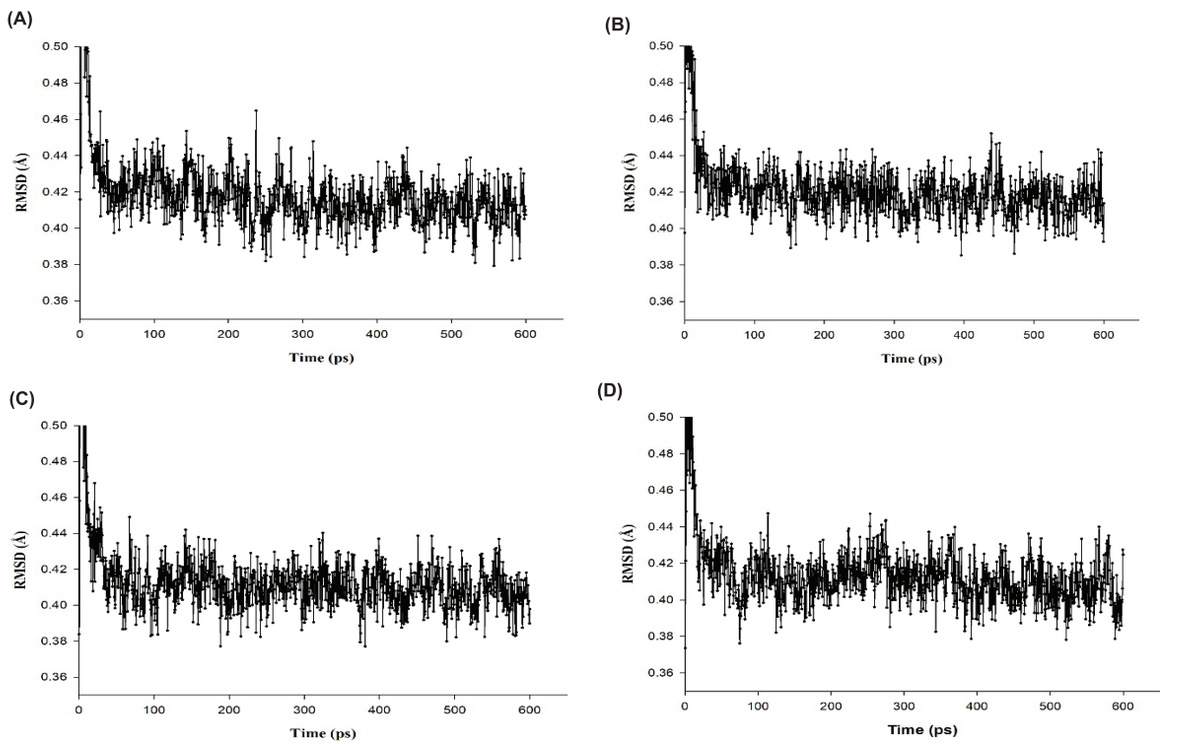

Fig. 12. RMSD of NMDA - Dihydroisotanshinone II (A), BACE1 - Dihydroisotanshinone II (B), BuChE - Dihydroisotanshinone II (C), and AChE - Dihydroisotanshinone II (D) complexes during 600 ps of molecular dynamics simulation.

4. Discussion

Alzheimer's disease, with its complex multifactorial pathophysiology, poses a significant challenge in terms of management. Therefore, it is imperative to explore multiple therapeutic strategies for Alzheimer's disease. Potential targets for Alzheimer's disease treatment include AChE, BuChE, BACE1, and NMDA receptors (NMDARs). This study focuses on compounds derived from *S. miltiorrhiza* that demonstrate the potential to inhibit most, if not all, of these target proteins.

Salvia miltiorrhiza Bunge, commonly known as danshen or red sage, holds a prominent place in traditional herbal medicine. Several studies have indicated that *S. miltiorrhiza* possesses neuroprotective properties relevant to Alzheimer's disease. Aqueous extracts of *S. miltiorrhiza* have demonstrated protection against neurotoxicity induced by Aβ25-35 in SH-SY5Y cells by reducing oxidative stress and mitigating the mitochondria-dependent apoptotic pathway [16]. Additionally, these extracts have been shown to block NMDA-evoked currents in whole-cell patch-clamp experiments [17].

In our research, we conducted docking simulations of 30 compounds from the medicinal herb *S. miltiorrhiza* with four proteins: AChE, BuChE, BACE1, and NMDAR to evaluate their potential to simultaneously inhibit all these proteins. Following the docking process, six compounds were identified that exhibited the ability to inhibit all four target proteins. Pharmacokinetic and toxicological predictions (ADMET) revealed that five of these six compounds possessed favourable pharmacokinetic properties, could cross the blood-brain barrier, were well-absorbed in the intestine, and did not induce skin irritation. These five compounds were Tanshinone I, Tanshinone IIA, 4-Methylenemiltirone, Isotanshinone I, Dihydroisotanshinone I, and Dihydroisotanshinone II. Furthermore, molecular dynamics simulations indicated that all five of these compounds maintained stable docking poses with the four target proteins. However, some potential risks, such as AMES toxicity, hepatotoxicity, and skin sensitisation, should be considered. Therefore, further *in vivo* or *in vitro* studies are necessary to validate and test the accuracy of these predictions.

Tanshinone I displayed strong interactions with all four target proteins, as evidenced by its negative binding energies with NMDA, BACE1, BuChE, and AChE, measuring -9.4, -10.5, -9.8, and -11.3 kcal/mol, respectively. In addition to the previously mentioned important amino acids of NMDA, this compound also interacted with PHE 250, ARG 131, and PHE 92, binds to BuChE through key amino acids, including PHE 329, SER 198, and GLY 116. Tanshinone I met all the requirements of Lipinski's rule of five. Moreover, it demonstrated the potential to cross the blood-brain barrier (Table 5). However, it exhibited AMES toxicity, as indicated by the ADMET profile.

Tanshinone IIA exhibited the potential to inhibit NMDA, BACE1, BuChE, and AChE due to its free binding energies with these proteins, which were -9.4, -10.3, -10.1, and -11.2 kcal/mol, respectively. In contrast to Tanshinone I, Tanshinone IIA did not exhibit any form of toxicity. Previous research indicated that Tanshinone IIA, at a dose of 1 μg/g, played a neuroprotective role, potentially related to decreased [Ca^{2+}] aggregation, alterations in NMDA receptor expression, and inhibition of calcium transportation [18-20]. It was reported that both Tanshinone I and Tanshinone IIA improved memory deficits induced by scopolamine (1 mg/kg, i.p.) in a mouse model (the passive avoidance test) by enhancing cholinergic signalling [21].

Isotanshinone I potentially inhibited all four target proteins, including NMDA, BACE1, BuChE, and AChE, due to its lower binding energy compared to reference drugs (-9.9, -10.6, -9.9, and -11.1 kcal/mol, respectively). However, according to ADMET profile results, it exhibited both AMES toxicity and hepatotoxicity. Isotanshinone I also interacted with some important amino acids previously identified in other studies, such as its interaction with ASP 32 of BACE1 and various important amino acids of BuChE, including GLY 16, PHE 329, and SER 198.

Dihydroisotanshinone I demonstrated strong interactions with all four target proteins, as evidenced by its negative binding energies with NMDA, BACE1, BuChE, and AChE, measuring -10.3, -10.6, -10.3, and -11.9 kcal/mol, respectively. Similar to Tanshinone I, Dihydroisotanshinone I exhibited AMES toxicity but did not show hepatotoxicity or skin sensitisation. Accumulated studies have primarily focused on the interaction between Dihydroisotanshinone I and AChE, a well-established anti-Alzheimer's disease target. Dihydroisotanshinone I is a high-affinity inhibitor of human AChE (Ki=0.6-0.8 μM). In a non-cell-based enzymatic assay, it inhibited AChE activities with an IC_{50} of 1.0 and 25 μM. Another study demonstrated that Dihydroisotanshinone I inhibited brain AChE and BuChE with IC_{50} values of 0.89 and 5.51 μM, respectively. *In vivo*, Dihydroisotanshinone I improved learning and memory impairments in mice induced by scopolamine, partially mediated by AChE inhibition [22].

Dihydroisotanshinone II potentially inhibited NMDA, BACE1, BuChE, and AChE, as indicated by its binding energies with these proteins, which were -10.4, -10.4, -10.3, and -11.1 kcal/mol, respectively. Dihydroisotanshinone II also interacted with PHE 250 of NMDA, an important amino acid mentioned earlier. Similar to Tanshinone IIA, Dihydroisotanshinone II did not exhibit any form of toxicity. It appears that there have been limited studies conducted on the potential of dihydroisotanshinone II in Alzheimer's disease treatment. Therefore, based on the results of this study, dihydroisotanshinone II could be a promising bioactive compound that warrants further investigation for the treatment of Alzheimer's disease.

It is noteworthy that the interactions between these five compounds and the active site residues significantly contributed to their binding energy with target proteins. Firstly, these compounds also interacted with important amino acids similar to those identified in previous studies. Secondly, hydrogen bonds and π-stacking interactions were the most prominent interactions observed in ligand-protein complexes in this study. Hydrogen bonds, as reported in previous studies, are the second most frequent type of interaction in various ligand-protein complexes [23]. They are known to significantly enhance the binding affinity between ligands and proteins. In this study, compounds formed hydrogen bond interactions with certain amino acids, such as Tanshinone I with ARG 131 of NMDA or Tanshinone I with ASP 62 of BACE1, and

SER 198. In addition to hydrogen bonds, π-stacking interactions were also observed in many ligand-protein complexes in this study. π-Stacking interactions also referred to as aromatic interactions, play a crucial role in ligand-protein recognition and drug design. They rank as the third most frequent interactions in ligand-protein complexes [23]. Evidence suggests that the formation of π-stacking interactions enhances the binding affinity of inhibitors for their targets. In our study, compounds exhibited π-stacking interactions with certain amino acids, such as Tanshinone IIA with TYR 184. π-π stacking interactions can be categorised into three types: edge-to-face stacked (T-shaped), offset stacked, and face-to-surface stacked [24]. T-shaped π-π stacking interactions were observed in various ligand-protein complexes in this study. For example, Tanshinone I formed T-shaped π-π stacking interactions with TYR 60 and TRP 277. This interaction was also observed in the Dihydroisotanshinone II-NMDA complex. Besides hydrogen bonds and π-π stacking interactions, compounds in this study also exhibited various other interactions with target proteins, such as amide- π stacked interaction, van der Waals, or pi-alkyl interaction. All of these interactions contributed to the binding energy of ligand-protein complexes. However, it should be noted that these interactions are not the sole determinants of binding affinity.

5. Conclusions

In this study, we found five natural compounds in *S. miltiorrhiza* Bunge with significant potential for Alzheimer's disease inhibition, utilising molecular docking and molecular dynamics simulations. All five compounds, namely Tanshinone I, Tanshinone IIA, Isotanshinone I, Dihydroisotanshinone I, and Dihydroisotanshinone II, exhibit drug-like properties, good absorption capabilities, and the potential to penetrate the blood-brain barrier.

CRediT author statement

Tung Bui Thanh: Conceptualisation, Design, Supervision, Critical Reviews; Trang Vu Dai: Design, Resources, Literature Search, Writing; Huong Le Thi: Resources, Literature Search, Writing.

COMPETING INTERESTS

The authors declare that there is no conflict of interest regarding the publication of this article.

REFERENCES

[1] Alzheimer's Association (2021), "2021 Alzheimer's disease facts and figures", *Alzheimer's Dement.*, **17(3)**, pp.327-406, DOI: 10.1002/alz.12328.

[2] H. Nguyen, M. Zaragoza, N. Wussler, et al. (2020), ""I was confused about how to take care of mom because this disease is different everyday": Vietnamese American caregivers' understanding of Alzheimer's disease", *Journal of Cross-Cultural Gerontology*, **35(2)**, pp.217-234, DOI: 10.1007/s10823-020-09396-7.

[3] H.W. Klafki, M. Staufenbiel, J. Kornhuber, et al. (2006), "Therapeutic approaches to Alzheimer's disease", *Brain*, **129(11)**, pp.2840-2855, DOI: 10.1093/brain/awl280.

[4] M.B. Colovic, D.Z. Krstic, T.D.L. Pasti, et al. (2013), "Acetylcholinesterase inhibitors: Pharmacology and toxicology", *Curr. Neuropharmacol.*, **11(3)**, pp.315-335, DOI: 10.2174/1570159X11311030006.

[5] M. Mesulam, A. Guillozet, P. Shaw, et al. (2002), "Widely spread butyrylcholinesterase can hydrolyse acetylcholine in the normal and Alzheimer's brain", *Neurobiol. Dis.*, **9(1)**, pp.88-93, DOI: 10.1006/nbdi.2001.0462.

[6] V. Calsolaro, P. Edison (2016), "Neuroinflammation in Alzheimer's disease: Current evidence and future directions", *Alzheimer's Dement.*, **12(6)**, pp.719-732, DOI: 10.1016/j.jalz.2016.02.010.

[7] S.L. Cole, R. Vassar (2008), "The role of amyloid precursor protein processing by BACE1, the β-secretase, in Alzheimer disease pathophysiology", *J. Biol. Chem.*, **283(44)**, pp.29621-29615, DOI: 10.1074/jbc.R800015200.

[8] H. Hilpert, W. Guba, T.J. Woltering, et al. (2013), "Beta-secretase (BACE1) inhibitors with high *in vivo* efficacy suitable for clinical evaluation in Alzheimer's disease", *J. Med. Chem.*, **56(10)**, pp.3980-3995, DOI: 10.1021/jm400225m.

[9] F. Stanzione, I. Giangreco, J.C. Cole (2021), "Use of molecular docking computational tools in drug discovery", *Prog. Med. Chem.*, **60**, pp.273-343, DOI: 10.1016/bs.pmch.2021.01.004.

[10] T.T. Bui, T.T.H. Ta, B.K. Nguyen, et al. (2022), "Molecular docking and molecular dynamics approach to identify potential compounds in Huperzia squarrosa for treating Alzheimer's disease", *Journal of Complementary and Integrative Medicine*, **19(4)**, pp.955-965, DOI: 10.1515/jcim-2021-0462.

[11] Z. Xing, G. Bi, T. Li, et al. (2023), "Plant growth and the contents of major bioactive compounds of *Salvia miltiorrhiza* Bunge grown in Mississippi, United States", *Horticulturae*, **9(3)**, DOI: 10.3390/horticulturae9030310.

[12] M.A. Rogawski, G.L. Wenk (2003), "The neuropharmacological basis for the use of memantine in the treatment of Alzheimer's disease", *CNS Drug Rev.*, **9(3)**, pp.275-308, DOI: 10.1111/j.1527-3458.2003.tb00254.x.

[13] A.K. Desai, G.T. Grossberg (2005), "Rivastigmine for Alzheimer's disease", *Expert Rev. Neurother.*, **5(5)**, pp.563-580, DOI: 10.1586/14737175.5.5.563.

[14] G.T. Grossberg (2003), "Cholinesterase inhibitors for the treatment of Alzheimer's disease: Getting on and staying on", *Curr. Ther. Res. Clin. Exp.*, **64(4)**, pp.216-235, DOI: 10.1016/S0011-393X(03)00059-6.

[15] P.C. May, B.A. Willis, S.L. Lowe, et al. (2015), "The potent BACE1 inhibitor LY2886721 elicits robust central Abeta pharmacodynamic responses in mice, dogs, and humans", *J. Neurosci.*, **35(3)**, pp.1199-1210, DOI: 10.1523/JNEUROSCI.4129-14.2015.

[16] H. Yu, L. Yao, H. Zhou, et al. (2014), "Neuroprotection against Abeta25-35-induced apoptosis by *Salvia miltiorrhiza* extract in SH-SY5Y cells", *Neurochem. Int.*, **75**, pp.89-95, DOI: 10.1016/j.neuint.2014.06.001.

[17] X. Sun, L.N. Chan, X. Gong, et al. (2003), "N-methyl-D-aspartate receptor antagonist activity in traditional Chinese stroke medicines", *Neurosignals*, **12(1)**, pp.31-38, DOI: 10.1159/000068913.

[18] C. Dai, Y. Liu, Z. Dong (2017), "Tanshinone I alleviates motor and cognitive impairments via suppressing oxidative stress in the neonatal rats after hypoxic-ischemic brain damage", *Mol. Brain*, **10(1)**, DOI: 10.1186/s13041-017-0332-9.

[19] M. Hei, F. Liu, Y. Luo (2010), "[Effect of Tanshinone IIA on phosphorylated NMDA receptor 1 expression and intracellular free calcium concentration in neonatal SD rats with hypoxic ischemic brain damage]", *Zhong Nan Da Xue Xue Bao Yi Xue Ban*, **35(9)**, pp.940-946, DOI: 10.3969/j.issn.1672-7347.2010.09.007.

[20] M. Hei, Y. Luo, X. Zhang, et al. (2011), "Tanshinone IIa alleviates the biochemical changes associated with hypoxic ischemic brain damage in a rat model", *Phytother. Res.*, **25(12)**, pp.1865-1869, DOI: 10.1002/ptr.3500.

[21] M. Ozarowski, P.L. Mikolajczak, A. Piasecka, et al. (2017), "Effect of *Salvia miltiorrhiza* root extract on brain acetylcholinesterase and butyrylcholinesterase activities, their mRNA levels and memory evaluation in rats", *Physiol. Behav.*, **173**, pp.223-230, DOI: 10.1016/j.physbeh.2017.02.019.

[22] X. Chen, J. Yu, B. Zhong, et al. (2019), "Pharmacological activities of dihydrotanshinone I, a natural product from *Salvia miltiorrhiza* Bunge", *Pharmacol. Res.*, **145**, DOI: 10.1016/j.phrs.2019.104254.

[23] R.F.D. Freitas, M. Schapira (2017), "A systematic analysis of atomic protein-ligand interactions in the PDB", *MedChemComm*, **8(10)**, pp.1970-1981, DOI: 10.1039/c7md00381a.

[24] W.R. Zhuang, Y. Wang, P.F. Cui, et al. (2019), "Applications of pi-pi stacking interactions in the design of drug-delivery systems", *J. Control Release*, **294**, pp.311-326, DOI: 10.1016/j.jconrel.2018.12.014.